Density functional study on the morphology and photoabsorption of CdSe nanoclusters

Del Ben, M ; Havenith, R W A ; Broer, R ; Stener, M

Abstract: The geometrical and electronic structures of a series of small CdSe quantum dots protected by various ligands have been studied by density functional theory. UV-vis spectra have been calculated by time-dependent density functional theory (TDDFT). The goal of this investigation is the rationalization of the basic properties of these systems, in particular, the nature of the exciton peaks. This study has been focused on the (CdSe)(x), x = 13, 19, 33, and 66, "magic-size" clusters that are characterized by high stability and large optical gaps. The geometries of the cluster are relaxed both in vacuum and in the presence of the surfactant ligands. To describe the interaction between the bare clusters and the surfactants, model types of ligands are introduced: fatty acids are modeled using formic and acetic acid and amines are modeled using ammonia and methyl amine. Present calculations demonstrate that the ligands play a crucial role in stabilizing the structure in a bulklike geometry and strongly affect the optical gap of the clusters, due to an optimal coordination of the surface atoms. For these "magic-size" clusters, the UV-vis spectrum is calculated at the TDDFT level. The calculated spectra are in good agreement with the experimental ones for clusters with the same dimension capped with the same type of Uganda. This suggests that our structures are realistic models of the actual quantum dots.

DOI: https://doi.org/10.1021/jp203686a

Density Functional Study on Morphology and Photoabsorption of CdSe Nanoclusters

Mauro Del Ben,[†] Remco W. A. Havenith,[‡] Ria Broer,[‡] and Mauro Stener[*,¶,§]

Institute of Physical Chemistry, University of Zürich, Switzerland,

Zernike Institute for Advanced Materials, University of Groningen, The Netherlands, and

Department of Chemical Sciences, University of Trieste, Italy

E-mail: stener@univ.trieste.it

[*]To whom correspondence should be addressed

[†]Institute of Physical Chemistry, University of Zürich, Winterthurerstrasse 190, CH-8057 Zurich, Switzerland

[‡]Department of Theoretical Chemistry, Zernike Institute for Advanced Materials, University of Groningen, Nijenborgh 4, 9747AG Groningen, The Netherlands

[¶]Department of Chemical Sciences, University of Trieste, Via Licio Giorgieri, 1 I-34127 Trieste - Italy

[§]Consorzio Interuniversitario Nazionale per la Scienza e Tecnologia dei Materiali, INSTM, Unità di Trieste

Abstract

The geometrical and electronic structures of a series of small CdSe quantum dots protected by various ligands have been studied by density functional theory. UV-Vis spectra have been calculated by Time Dependent Density Functional Theory. The goal of this investigation is the rationalization of the basic properties of these systems, in particular the nature of the exciton peaks. This study has been focused on the $(CdSe)_x$, x=13, 19, 33 and 66, "magic size" clusters which are characterized by high stability and large optical gap. The geometries of the cluster are relaxed both in vacuum and in the presence of the surfactant ligands. To describe the interaction between the bare clusters and the surfactants, model types of ligands are introduced: fatty acids are modelled using formic and acetic acid, amines are modelled using ammonia and methyl amine. Present calculations demonstrate that the ligands play a crucial role in stabilizing the structure in a bulk like geometry, and strongly affect the optical gap of the clusters, due to a optimally coordination of the surface atoms. For this "magic-size" clusters the UV-Vis spectrum is calculated at the TDDFT level. The calculated spectra are in good agreement with the experimental ones for clusters with the same dimension capped with the same type of ligands. This suggests that our structures are realistic models of the actual quantum dots.

Introduction

Colloidal quantum dots (QDs) represent one of the most interesting and studied system in the field of semiconductor nanocrystals, in particular because, due to the quantum confinement effect, their electronic and optical properties are strongly size dependent[1]. In this respect, CdSe has been one of the most studied II-VI dots due to the ease of synthesis, and the fact that, according to the dimension of the QDs, its optical gap can cover all the visible spectrum[2].

In general the QDs can be divided into two regions, the core, made by a semiconductor nanocrystal and the passivating ligands at the surface, such as fatty acids, thiolates and various amines. These surface ligands are fundamental for enhancing the solubility of the QDs in various solvents, in stabilizing the core structure and can strongly affect the electronic and spectroscopic properties of the QDs.

The rational modeling of the surface of the QD nanocrystals is of great interest: in this respect accurate theoretical description of its structure as well as optical and electronic properties of QDs is central topic for the application of these systems as building blocks for nanostructured materials. Moreover the effective-mass approximation[3], which is often employed to describe the exciton confinement in analogy to the particle in a box model, was found to diverge from the experimental results for small particle sizes, thus requiring a more accurate approach.

The aim of this work is to employ density functional theory (DFT) to provide detailed information on the structure, electronic properties, and optical absorption of small CdSe quantum dots capped by different types and numbers of ligands. The goal of these calculations is to understand of the basic properties of these systems, in particular the nature of the exciton peak. In this respect, the UV-Vis absorption spectrum of model systems has been calculated at the Time Dependent Density Functional Theory (TDDFT) level, providing an accurate (state of art) theoretical description of the exciton phenomena. In this way, it is possible to analyze the charge redistribution involved in these excitations, and so, going beyond the effective mass model, to a better description of the spectroscopic properties of the quantum dots[4–7].

Although the problem addressed by the present work is quite general, there are other aspects

related to the CdSe quantum dots which have not been considered here and would be suitable for further investigations. In particular a very important problem is related to the growth phenomenon, which could be tackled by means of a suitable computational scheme.

The model clusters, used to reproduce the real nanocrystals, have been designed taking into account experimental information on the structure[8,9], the reaction mechanism of formation[10,11] and surface passivation[12–15] of semiconductor nanocrystals. The present work has been focused of the $(CdSe)_{33}$ cluster which is the smallest CdSe nanocrystal isolated and characterized by mass spectrometry[16,17]. For this cluster, the UV-Vis absorption spectrum is experimentally available (Figure 10a) and it has been employed as a benchmark to test the model systems[2,16,18].

Recently, magic size cysteine-capped CdSe nanoparticles have been synthesized in aqueous solution at room temperature[19,20]. The CdSe nanoparticles were identified as selective grown, water soluble $(CdSe)_{33}$ and $(CdSe)_{34}$ clusters with diameter of ca. 1.57 nm. The collected UV-Vis absorption spectra show very similar features to those obtained for the colloidal mixture of decylamine-capped $(CdSe)_{33}$ and $(CdSe)_{34}$ clusters synthesized in toluene[16]. This can be interpreted as a low influence of the surfactant ligands on the UV-Vis absorption spectrum for this small magic size nanoparticles.

A detailed computational investigation on the effect of the ligands on the electronic properties of the $(CdSe)_{33}$ cluster has just been reported by Kilina et al.[4]. In that work methyl amine and trimethylphosphine oxide (used to reproduce the trioctylphosphine oxide (TOPO) surfactant) have been employed as model ligands. Therefore also in the present work we have chosen ammonia and methyl amine as protecting ligands. Carboxylic acids have also been considered previously as model ligands[21], here we propose that the coordination of the acids passes through the dissociation of the O-H bond. In this way the the carboxylate coordinates a surface Cd atom, while the hydrogen saturates a Se atom. The effect related to this kind of surface passivation on the electronic properties and absorption spectra of the CdSe clusters is the main purpose of this work.

The effect of bioconjugation of $(CdSe)_n$ clusters with Adenine has been also recently considered in a computational work, in terms of geometry, electronic structure and electronic spectra[22].

Very recently, an extended study on the structural and optical properties of CdSe nanoclusters has been published[23] for large sizes up to $(CdSe)_{54}$. An intensive structural search has been employed to identify the most relevant low energy isomers as well as their tiny energetic differences. In that work also optical properties were considered, but only within a rather narrow excitation energy range (around 0.5 eV) so that only the first more prominent spectral feature could be described. In the present work we have been able to extend the excitation energy range up to 1 eV or more thanks to the efficient implementation of the TDDFT algorithm in the ADF code. Moreover in ref[23] the cluster structures considered were subject to symmetry constraints, which we found better to remove in present work.

Our choice is supported by a previous study on the mechanism of the formation of CdSe nanocrystals in high boiling point solvents with long alkane chains and without the use of trialkylphosphine as a surfactant for the chalcogenide[11]. There are evidences that, in the case of CdSe nanocrystal synthesis, a redox reaction takes place in the long alkane chain solvents: Se is reduced to H_2Se gas and concomitantly the long alkane chains are oxidated to alkene chains; then, the Cd carboxylate complex reacts with H_2Se to form CdSe nanocrystals. It is possible to speculate, from the proposed mechanism, that the coordinated groups at the surface are probably carboxylate for the cadmium and hydrogen for the selenium.

Although these semiconductor clusters are the smallest nanocrystals that can be isolated experimentally, they are built up of hundreds of atoms. So, from a computational point of view, these systems are still challenging and their modeling needs high performance computing and efficient quantum chemistry computer codes. In these terms the aim of this investigation is to reach that region of nanometric size that opens the opportunity to study quantum confinement effects in realistic models of QDs.

Model Clusters and Computational Scheme

In this work only wurtzite structures have been considered. Although for very small clusters alternative structures are of course possible, the wurtzite structure is the most common structure observed in CdSe nanoclusters, and is often assumed in computational studies where model clusters are employed. For example in reference[11] an alternative route to zinc-blend structure synthesis of CdSe nanocluster is considered as an exception if compared to wurtzite structures. For this reason we believe that the findings obtained with cluster models with only wurtzite structure are already significant and it is not necessary to consider clusters with alternative structures.

Bare Clusters

The initial structures of the CdSe bare clusters, which will be employed as starting point for the following geometry optimization, are built according to the following procedure:

- Only stoichiometric CdSe clusters are taken into account.
- The cluster is built by cutting an almost spherical portion of the wurtzite lattice with bulk Cd-Se bond lengths. The analogous construction of CdSe clusters from the bulk semiconductor has been used in previous theoretical studies[4,5,24].
- The bare clusters are chosen such that the overall point group of the structures is C_{3v}. This means that the origin of the cluster has to lie on one of the two C_3 axis of the wurtzite bulk structure. These two axes are both parallel to the c axis, one contains the Cd-Se bond, the other passes on the barycenter of three nearest neighbor Cd (or Se) atoms, belonging to the same (001) plane but not to the same tetrahedral block.
- The number of formula units for the bare clusters is chosen according to the magic-size series reported by Kasuya et al.[16], that is $(CdSe)_n$, n=13, 19 and 33. In addition also the 66 formula units cluster has been built to reproduce nanoparticles of $\sim$17 Å diameter.

- To obtain the $(CdSe)_n$, n=13, 19, 33, 66 clusters cutting the wurtzite structure, the centers of the clusters have been chosen as follows:
  - O1≡(0,0,0) on a selenium atom for $(CdSe)_{13}$ and $(CdSe)_{19}$
  - O2≡$(a/3,a/3,u/2)$ the point at the center of the octahedral cage of the wurtzite structure for $(CdSe)_{33}$
  - O3≡$(0,0,(u+c)/2)$ the midpoint of a next nearest Cd and Se along the c axes for $(CdSe)_{66}$

  Where u is the bulk bond length, a and c are the lattice parameters of the wurtzite structure.

Ligands

In the bare clusters two kinds of surface atoms can interact with ligands[4,25]. Focusing on the cadmium atoms , which were shown to have the dominant binding interaction with oxygen and nitrogen of the model ligands[21], these two typologies are: two-coordinated Cd atoms, that are bounded to only two Se atoms, having two dangling bonds; and three-coordinated Cd atoms that are bound to three Se atoms, having one dangling bond. Previous calculations have shown that one-coordinated Cd atoms are not stable with respect to dissociation[25], so they have not been considered.

A characteristic of the surface atoms of the $(CdSe)_{33}$ and $(CdSe)_{66}$ bare clusters is that they are built in such a way that the number of three- and two-coordinated Cd atoms is the same as the number of three- and two-coordinated Se atoms.

The two-coordinated Cd atoms are expected to be less tightly bound than three-coordinated ones because of the higher number of dangling bonds. This assumption is supported by the calculations on the CdSe bare clusters, reported by Pudzer et al.[5]. In this paper it is shown that CdSe nanoparticles with ideal wurtzite structures are quasi-metallic, due to the dangling bonds present at the surface. Geometry relaxation leads to a final geometry with only three-coordinated interfacial atoms, concomitantly with an opening of the gap of the clusters.

Therefore it is assumed that the ligands saturate the surface atoms starting with those with the maximum number of dangling bonds. This is also consistent with the XPS studies showing that not all surface atoms interact with ligands[13].

To simulate the interaction between the bare clusters and the surfactants, model types of ligands are introduced. These models have to mimic, as much as possible, the real ligands used in the ordinary synthesis (i.e. fatty acid, amines, ...). The model surfactants that have been considered are:

- Carboxylates, which are modeled using formic acid. In this case the formate anion is placed near all two-coordinated Cd atoms, at an initial distance taken from the experimental distance of the cadmium acetate salt. The O-C-O plane is oriented orthogonal to the Se-Cd-Se plane in order to emulate a tetrahedral coordination. At the same time, hydrogen is placed near all two-coordinated Se atoms, orthogonal to the Cd-Se-Cd plane, at a distance taken from the experimental H_2Se bond length. In the case of the $(CdSe)_{33}$ cluster also acetate has been used.

- Amines, which are modelled using ammonia placed near all two-coordinated Cd atoms. In the case of the $(CdSe)_{33}$ cluster also the effect of the passivation of the three-coordinated Cd atoms and the use of methyl amine instead of ammonia have been considered.

- Both fatty acids and amines together as surfactants, which are reproduced using formate-hydrogen pair to saturate the two-coordinated atoms and ammonia for the three-coordinated Cd atoms.

Cluster Geometry Optimization

After the initial cluster geometry is built, using the protocol described in the two previous subsections, a relaxation procedure is required to get the final cluster structure to the nearest energy minimum.

This procedure is a common routine used in all previous calculations on CdSe clusters[4,5,7,25], and has the main purpose of reconstructing the surface atoms in order to saturate their dangling bonds.

Preliminary calculations, that have been performed constraining the C_{3v} symmetry, have shown that this constraint leads to non optimally saturation of the two-coordinated Se atom by hydrogen. Therefore the geometry optimization were carried out without any symmetry constrains, even if the final relaxed structures resemble closely a C_{3v} or C_3 arrangement.

Computational Details

All calculations have been performed using the parallel Amsterdam Density Functional code (ADF)[26].

- The following Slater Type Orbitals (STO) basis sets have been employed:
  - Cadmium: Double Zeta (DZ) 3d frozen
  - Selenium: DZ 3p frozen
  - Oxygen, Carbon, Nitrogen and Hydrogen: Triple Zeta with polarization (TZP)
- XC model potential:
  - In geometry optimizations: Local Density Approximation (LDA), functional of Vosko, Wilk and Nusair (VWN[27])
  - For the TDDFT calculations: Generalized Gradient Approximation (GGA), functional of Perdew-Wang (PW91[28])

The 3d and 3p frozen wording means that all the atomic orbitals that have their energy below that shell are treated as core frozen orbitals.

Basis set size is consistent with two previous work on CdSe clusters[4,23]. This choice has been also checked by enlarging the basis set to TZP for Cd and Se without observing relevant differences

in the results

The convergence criteria of the geometry optimizations have been kept fixed to their default values.

The choice to employ the LDA VWN functional for geometry optimization is justified by the excellent agreement between Cd-Se interatomic distances of the core structure of the cluster optimized at the LDA VWN level with respect to the experimental bulk value. In fact, for the large $(CdSe)_{66}$ protected by formate ligands, we obtained an optimized value of 2.641 Å which is in fairly nice agreement with the experimental bulk value of 2.632 Å. It is worth noting that the LDA approximation has been already successfully employed in a previous work to optimize the structures of CdSe nanoclusters[5]. On the other hand, the choice of the functional in the TDDFT calculations is not a trivial task. In fact, it is generally accepted that, at least for small molecules, the asymptotic correction, like in LB94[29] is important to obtain good excitation energies and the proper description of Rydberg orbitals. In the present case, however, Rydberg states are unimportant so we decided to employ a more standard GGA functional like PW91. Anyway, when a calculated spectrum is compared with an experiment, the most important aspect to be considered is the intensity distribution, rather than absolute excitation energies. The latter can be pragmatically fixed by a proper energy shift of the whole spectrum.

The band structure calculation has been performed employing the BAND code that is a periodic structure program for the study of bulk crystals, polymers, and surfaces, as part of the ADF package[30]. The numerical integration scheme for the k-space integrals used 196 symmetry-unique sample points in the irreducible wedge of the Brillouin zone.

Furthermore, all the TDDFT spectra have been broadened by Gaussian functions with constant σ=0.06 eV.

Results and Discussion

Optimized Structures

Bare Clusters

For the smaller clusters (n=13, 19 and 33) the optimized geometries of the bare structures have been calculated. It has not been possible for the biggest one (n=66), due to the high computational effort required. In fact the main problem in these optimizations is the quasi-metallic behavior of the starting wurtzite geometry, that involves the presence of two coordinated Cd atoms at the surface. This is mostly due to the non-saturated valencies of the Cd atoms and leads to a smear of the electrons at the edge. Only once the optimization is performed and all the dangling bonds have been saturated, the electronic configuration of the clusters exhibit the typical HOMO-LUMO gap expected for a semiconductor species[5].

Figure 1 compares the calculated relaxed geometries with the corresponding ideal wurtzite structure. The surface of each cluster undergoes a strong reconstruction, while the wurtzite core is maintained.

The structural data, obtained from the geometry optimization on the bare clusters, are briefly reported in Table 1. In general, the bare clusters exhibit, for the Cd-Se bonds in the center of the quantum dot, a value longer than that in the bulk material, while optimized bonds between Cd and Se atoms on the surface are slightly shorter than those in the nanocrystal core (-0.7% in the case of $(CdSe)_{33}$). This is related to the surface reconstruction and can be explained according to the less coordinative environment for the surface atoms that results in closer positioning for Se and Cd.

As it is possible to notice in Figure 1, there is a different geometrical reorganization for the surface cadmium and selenium atoms, whereas, in both cases the fully coordinated atoms resemble the ideal tetrahedral disposition of the wurtzite structure. Cadmium atoms exhibit the tendency of being pulled into the plane formed by its three coordinating selenium atoms. In this way, its geometrical surrounding is close to a planar trigonal coordination. On the other hand selenium reconstructs puckering out, forming a coordination structure that resembles a pyramidal geometry.

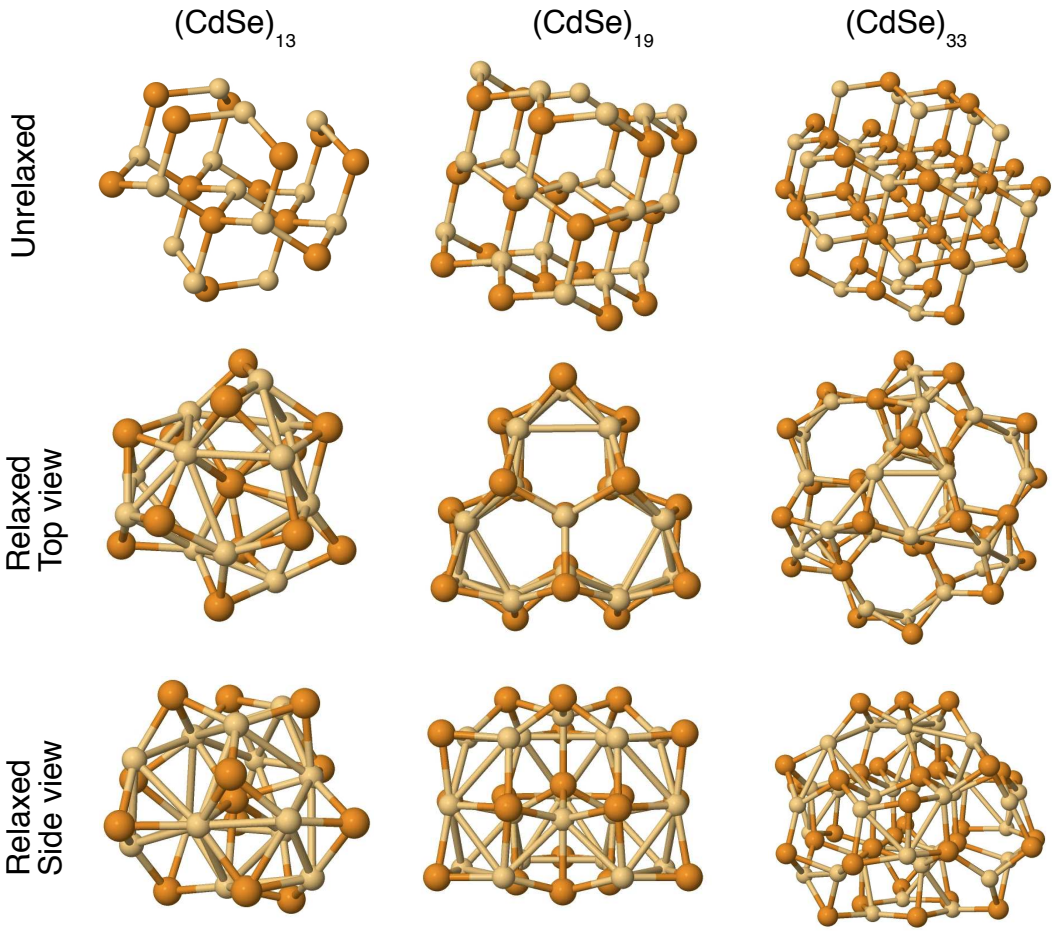

Figure 1: Unrelaxed and relaxed wurtzite structure of $(CdSe)_n$, n=13, 19, and 33. The Cd is light yellow and the Se is bronze in the ball and stick models. The side view is parallel to the c axis, the top view is along the c axis.

Due to this behavior the average bond angle for the surface Cd atoms is close to 120°, whereas the average bond angle for the Se surface atoms is around 90° (Table 1). These reconstructions are similar to the relaxation observed for bulk CdSe (001) surface[31].

Deglmann et. al. have studied the structure of small semiconductor clusters, composed of few formula units (up to the heptamer)[25]. In the case of the dimers, $(CdSe)_2$, six minima on the potential surface have been found, similar motifs appear on the relaxed surface of the clusters treated in this work. This suggests that, in general, surface reconstruction occurs quite independent from the core relaxation.

Table 1: Average bond lengths and angles for the bare CdSe optimized clusters. (4) = four-coordinated atoms, (3) =three-coordinated atoms. No two-coordinated atoms have been observed in the relaxed structures, four-coordinated atoms can lie at the cluster surface. The gap is defined as the HOMO - LUMO energy difference (the GGA gap is calculated using the geometry obtained from the structural relaxation performed employing LDA for the exchange correlation functional). Experimental CdSe bulk bond length 2.632 Å; tetrahedral angle.

System	Surface Atoms	Property		LDA	GGA
$(CdSe)_{13}$	96%	Bond Length (Å)	Cd(4)-Se	2.718	
			Cd(3)-Se	2.648	
		Angle (deg)	Se-Cd(4)-Se	108.8	
			Se-Cd(3)-Se	118.3	
			Cd-Se(4)-Cd	85.2	
			Cd-Se(3)-Cd	85.0	
		Gap (eV)		2.56	2.66
$(CdSe)_{19}$	89%	Bond Length (Å)	Cd(4)-Se	2.699	
			Cd(3)-Se	2.618	
		Angle (deg)	Se-Cd(4)-Se	110.0	
			Se-Cd(3)-Se	117.0	
			Cd-Se(4)-Cd	97.2	
			Cd-Se(3)-Cd	87.3	
		Gap (eV)		1.80	1.90
$(CdSe)_{33}$	64%	Bond Length (Å)	Cd(4)-Se	2.676	
			Cd(3)-Se	2.613	
		Angle (deg)	Se-Cd(4)-Se	109.3	
			Se-Cd(3)-Se	117.9	
			Cd-Se(4)-Cd	108.1	
			Cd-Se(3)-Cd	89.6	
		Gap (eV)		1.67	1.74

Capped Clusters

The presence of the ligands allows the saturation of the dangling bonds by passivating the active sites on the surface. In this case, in fact, the unpaired electron on the surface becomes part of the bonds between the surfactant molecule and the interfacial atoms.

The first consequence associated with the presence of the ligands is that the density of states for the clusters with the wurtzite ideal structure displays a clear HOMO-LUMO gap. This is not the case for the bare clusters that, for ideal wurtzite structure, exhibit a quasimetallic behavior. As

expected, this gap becomes wider when the dangling bonds are saturated by the ligands.

For $(CdSe)_{13}$ and $(CdSe)_{19}$ clusters, due to the small number of formula units, there is a strong surface reconstruction, compared to the ideal wurtzite structure, even in the presence of surface ligands. Both bare clusters have been built up, setting the origin of the systems on a selenium atom of the wurtzite lattice, resulting in a diameter of $\sim$8 Å and $\sim$10 Å respectively.

Figure 2 shows the relaxed structures achieved using as capping agent the formate hydrogen pair.

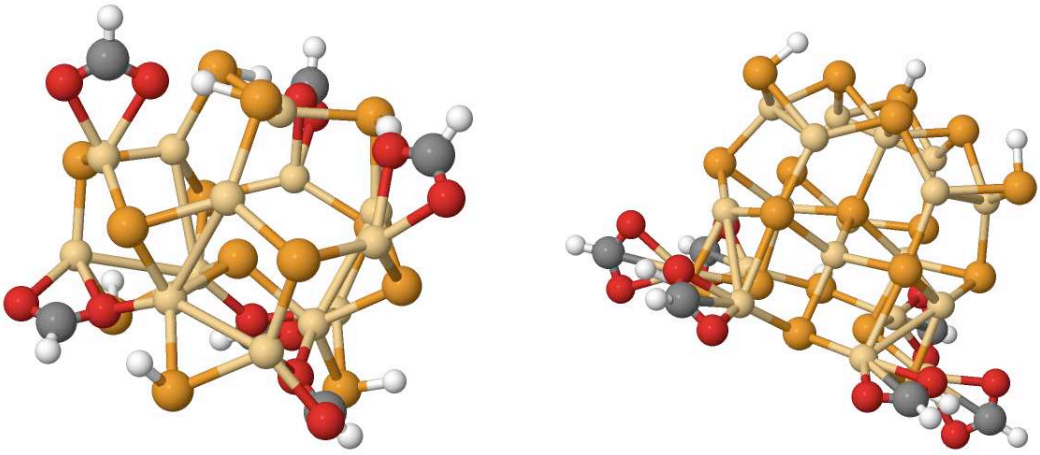

(a) (b)

Figure 2: Optimized structures used in modeling the $(CdSe)_{13}$ and $(CdSe)_{19}$ clusters capped by the formate-hydrogen pair. a) $(CdSe)_{13}$ with 6 formate-hydrogen pairs. b) $(CdSe)_{19}$ with 6 formate-hydrogen pairs.

The formate ligand saturates the two-coordinated Cd atoms giving rise to a tetrahedral coordination, both oxygens of the carboxylic group, generally, bind to the Cd atom with almost equal bond lengths. The average Cd-O bond length is around $\sim$2.3 Å, very close to that obtained experimentally for the cadmium formate salt (2.26 Å). The O-C-O plane is almost orthogonal to the Se-Cd-Se plane showing the tendency of cadmium to be tetrahedrally coordinated.

The formate ligand tends to move its oxygen atoms in the direction of electron-deficient sites, such as hydrogens (bound to a selenium) or other surface cadmium atoms. The average C-O bond length is 1.26 Å, and the average O-C-O angle is $\sim$123°, so there are no strong deviations from the structure of the formate anion due to the interaction between the ligand and the surface.

The coordination of hydrogen to a two-coordinated Se atom, resembles the geometry of the H_2Se molecule. In the clusters the average Se-H bond length is $\sim$1.5 Å, very close to the experimental value 1.49 Å of the H_2Se. The angle between the Se-H bond and the Cd-Se-Cd plane, is around 90°, similar to the value (91°) of the hydrogen selenide.

For the three-coordinated Cd and Se atoms not saturated by ligands, a similar behavior previously found for the bare clusters is observed, i.e. a trigonal planar coordination for the cadmium (Se-Cd-Se angle $\sim$120°), and a puckered coordination for the selenium (Cd-Se-Cd angle $\sim$90°).

A particular feature in the geometrical arrangement of the $(CdSe)_{19}$ capped cluster (Figure 2b) is that the formate ligands bind the cadmium atoms in two ways. The first is the usual observed in the case of the capped $(CdSe)_{13}$ clusters, with the O-C-O plane almost orthogonal to the Se-Cd-Se one. The second takes place when the cadmium, which the formate is bonded, due to the geometry relaxation, becomes a three-coordinated atom; in this case, the Cd-O bond lengths are no longer equal. The O-C-O plane turns in such a way that the smallest Cd-O bond results as the fourth coordination of an hypothetical tetrahedron around the Cd atom.

The $(CdSe)_{33}$ nanocrystal has been one of the most studied clusters, both in a passivated form, capped with different ligands[4,21], and in the bare form[5]. The bare $(CdSe)_{33}$ cluster is built up by placing the origin of the nearly spherical system on the center of an octahedral cage of the ideal wurtzite lattice (origin O2), resulting in a diameter of $\sim$13 Å. The unrelaxed $(CdSe)_{33}$ bare cluster has its number of two- and three-coordinated Cd atoms equal to the number of the two- and three-coordinated Se atoms. This means that there is only one way for the coordination of the paired ligands that consist of the saturation of all the two-coordinated atoms.

The used ligand arrangements are:

- 9 formate (one on each two-coordinated Cd atom) and 9 hydrogen (one on each two-coordinated Se atom) (Figure 3a).

- 9 acetate (one on each two-coordinated Cd atom) and 9 hydrogen (one on each two-coordinated Se atom) (Figure 3b).

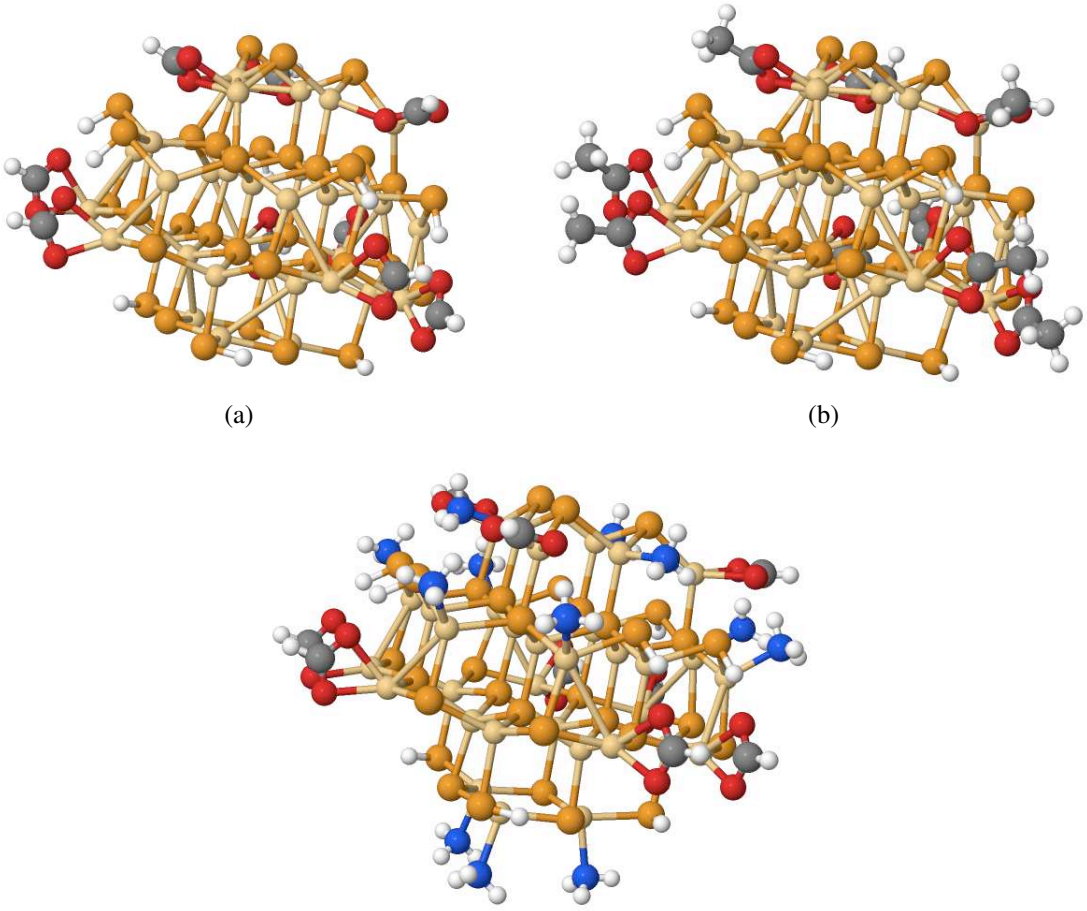

(a) (b)

(c)

Figure 3: Structures used in modeling the $(CdSe)_{33}$ cluster in which the two-coordinated atoms are capped with the paired ligands. a) $(CdSe)_{33}$ with 9 formate-hydrogen pairs. b) $(CdSe)_{33}$ with 9 acetate-hydrogen pairs. c) $(CdSe)_{33}$ with 9 formate-hydrogen pairs and 12 NH_3.

- 9 formate (one on each two-coordinated Cd atom), 9 hydrogen (one on each two-coordinated Se atom) and 12 NH_3 (one on each three-coordinated Cd atom) (Figure 3c).
- 9 NH_3 (one on each two-coordinated Cd atom) (Figure 4a).
- 9 methyl amines (one on each two-coordinated Cd atom) (Figure 4b).
- 12 NH_3 (one on each three-coordinated Cd atom) (Figure 4c).
- 9 NH_3 (one on each two-coordinated Cd atom) plus 12 NH_3 (one on each three-coordinated Cd atom) (Figure 4d).

The average structural data for the $(CdSe)_{33}$ cluster capped with the paired ligands are reported in Table 2; those related to the case of the donor ligands are summarized in Table 3.

Consider at first the difference between the cases in which only the carboxylate hydrogen pair is used as surfactant species. The structural changes, for the core CdSe part of the cluster, arising from the use of acetate instead of formate are negligible. This is clearly shown in the first part of Table 2, in fact, looking at the data that involve only Cd and Se atoms, they display only small differences (of the order of 0.001 Å in length or 0.1 degrees for the angles).

The only significant displacement in this case is related to the carboxylic group for which the Cd-O distance increases by $\sim$0.02 Å, and the O-C-O angle decreases by $\sim 3^\circ$ in passing from the formate to the acetate. Both these changes might be due to the steric effects related to the methyl group of the acetate ligand.

When, together with the formate-hydrogen pair, also ammonia is used, it is seen from Figure 3c, compared to Figure 3a, that there are no strong structural reorganizations of the local environment of the three-coordinated Cd atoms, on which the ammonia fragments are bonded. However, from an overall point of view, the presence of the NH_3 affects the coordination of the formate ligands, resulting in a more symmetric disposition of the surfactant molecules.

Table 2: Average bond lengths and angles for the $(CdSe)_{33}$ optimized clusters capped with paired ligands. In the table, (4) = four-coordinated atoms, (3) = three-coordinated atoms, (2) = two-coordinated atoms. In the case of the four-coordinated atoms if the value is not reported this means that the relaxed cluster does not contain such type of atoms. The angle Se-Cd-C-O is the dihedral angle formed by the Se-Cd-Se plane and the O-C-O plane; the CdSeCd-H angle is the dihedral angle formed by the plane Cd-Se-Cd and the Se-H bond. Experimental values: CdSe bulk bond length 2.632 Å, angle 109.5°; H_2Se bond length 1.49 Å, angle 91°; cadmium formate Cd-O bond length 2.26 Å.

System	Number and Type of Ligands	Property		LDA	GGA
$(CdSe)_{33}$	$9(HCOO^- / H^+)$	Bond Length (Å)	Cd(4)-Se	2.654	

Continued on next page

Table 2 Continued from previous page

			Cd(3)-Se	2.609	
			Cd(2)-Se	2.596	
(Figure 3a)			Cd(2)-O	2.318	
			Se(2)-H	1.505	
			C-O	1.262	
		Angle (deg)	Se-Cd(4)-Se	109.4	
			Se-Cd(3)-Se	119.0	
			Se-Cd(2)-Se	124.0	
			Cd-Se(4)-Cd	108.7	
			Cd-Se(3)-Cd	94.6	
			Cd-Se(2)-Cd	91.5	
			Se-Cd-C-O	88.1	
			CdSeCd-H	92.7	
			O-C-O	123.2	
		Gap (eV)		2.39	2.51
$(CdSe)_{33}$	$9(CH_3COO^- / H^+)$	Bond Length (Å)	Cd(4)-Se	2.656	
			Cd(3)-Se	2.610	
			Cd(2)-Se	2.596	
(Figure 3b)			Cd(2)-O	2.296	
			Se(2)-H	1.514	
			C-O	1.272	
		Angle (deg)	Se-Cd(4)-Se	109.3	

Continued on next page

Table 2 Continued from previous page

			Se-Cd(3)-Se	119.1	
			Se-Cd(2)-Se	124.5	
			Cd-Se(4)-Cd	108.7	
			Cd-Se(3)-Cd	94.1	
			Cd-Se(2)-Cd	91.9	
			Se-Cd-C-O	88.0	
			CdSeCd-H	92.2	
			O-C-O	120.7	
		Gap (eV)		2.38	2.50
$(CdSe)_{33}$	$9(HCOO^- / H^+)$	Bond Length (Å)	Cd(4)-Se	2.644	
	$12NH_3$		Cd(3)-Se	2.634	
			Cd(2)-Se	2.585	
(Figure 3c)			Cd(3)-N	2.320	
			Cd(2)-O	2.321	
			Se(2)-H	1.498	
			C-O	1.260	
		Angle (deg)	Se-Cd(4)-Se	109.3	
			Se-Cd(3)-Se	115.3	
			Se-Cd(2)-Se	125.9	
			Cd-Se(4)-Cd	109.2	
			Cd-Se(3)-Cd	98.2	
			Cd-Se(2)-Cd	101.9	

Continued on next page

Table 2 Continued from previous page

	Se-Cd-C-O	90.0	
	CdSeCd-H	95.0	
	O-C-O	123.6	
Gap (eV)		2.39	2.51

This ordering of the ligands at the surface suggests a mutual interaction between the oxygen of the carboxylic group and the hydrogen of the ammonia molecule. This conclusion has been achieved by looking at the orientation of the NH_3 molecules in the vicinity of a formate; in these cases, the ammonia is oriented such that one of its hydrogens points to the nearest carboxylic oxygen (Figure 3c).

When only ammonia or methyl amine molecules are used as surface ligands, as shown in Figure 4, the structure of the CdSe core part of the cluster resembles that of the bare $(CdSe)_{33}$ one (Figure 1). The first similarity is that all the surface atoms are 3- or four-coordinated atoms. Both ammonia and methyl amine ligands bind a three-coordinated Cd atom, with an average bond length of $\sim$2.3 Å. Their influence on the local environment of the Cd atom is weak compared to the bare cluster: in fact the three-coordinated Cd atoms remain almost in the usual trigonal coordination, and display only a limited puckering due to the ligand interaction.

The resemblance between the structures of the bare and the ammonia/amine capped clusters, shown in the Figures, can be better analyzed from the data reported in Table 1 and Table 3. The data in the Tables show that the average bond angles in the different cases are close to each other, with an average displacement less than 1°, this shows the overall resemblance of the structures. However, the average bond lengths are systematically larger for the Cd(3)-Se distances and shorter for the Cd(4)-Se distances, in the case of the capped clusters compared with the bare ones. This behavior is most pronounced for the cluster with all its surface cadmium atoms capped with ammonia.

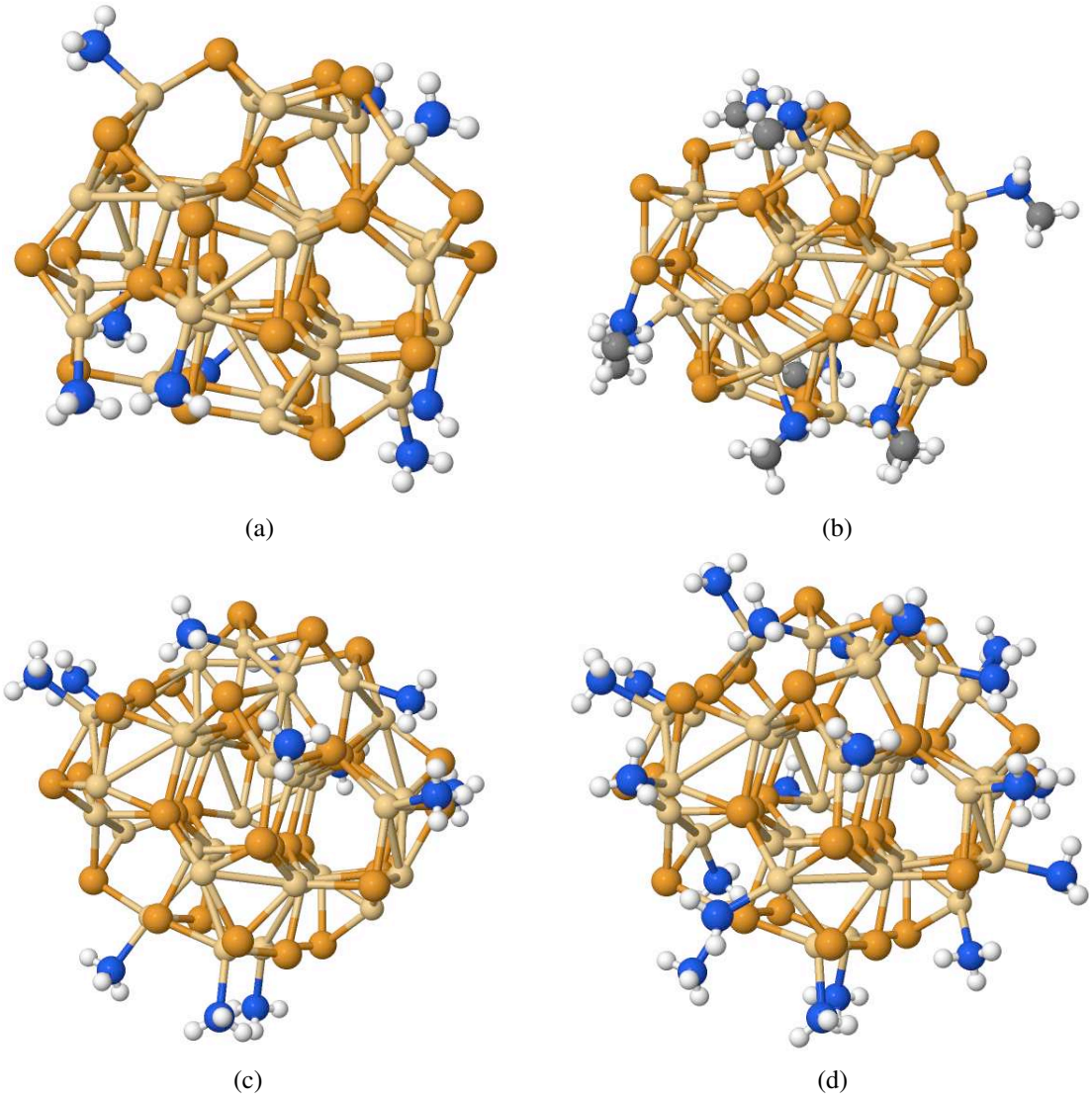

(a) (b)

(c) (d)

Figure 4: Structures used in modeling the $(CdSe)_{33}$ cluster in which only the surface cadmium atoms are capped whit ammonia or methyl-amine. a) $(CdSe)_{33}$ with 9 NH_3. b) $(CdSe)_{33}$ with 9 methyl-amines. c) $(CdSe)_{33}$ with 12 NH_3. d) $(CdSe)_{33}$ with 21 NH_3.

When the carboxylate-hydrogen pairs are used in capping the two-coordinated atoms, the HOMO-LUMO gap becomes wider by $\sim$0.5 eV than in the other cases. This can be related to the different mechanism of the ligands to saturate the surface dangling bonds, that is weaker for ammonia and stronger for the carboxylate-hydrogen pairs.

The higher efficiency of the formate and acetate groups can be due to electronic and geometric effects. The electronic effect displays the strong negative character of the oxygen in the carboxylic group; this can stabilize the partially positive unsaturated cadmium atoms better than the amino

Table 3: Average bond lengths and angles for the $(CdSe)_{33}$ optimized clusters capped with donor ligands. In the Table, (4) = four-coordinated atoms, (3) = three-coordinated atoms. All the relaxed structures do not display two-coordinated atoms.

System	Number and Type of Ligands	Property		LDA	GGA
$(CdSe)_{33}$	9 NH_3	Bond Length (Å)	Cd(4)-Se	2.666	
			Cd(3)-Se	2.634	
			Cd(3)-N	2.317	
(Figure 4a)		Angle (deg)	Se-Cd(4)-Se	109.3	
			Se-Cd(3)-Se	116.6	
			Cd-Se(4)-Cd	108.1	
			Cd-Se(3)-Cd	90.6	
		Gap (eV)		1.80	1.87
$(CdSe)_{33}$	9 CH_3NH_2	Bond Length (Å)	Cd(4)-Se	2.665	
			Cd(3)-Se	2.637	
			Cd(3)-N	2.312	
(Figure 4b)		Angle (deg)	Se-Cd(4)-Se	109.2	
			Se-Cd(3)-Se	116.7	
			Cd-Se(4)-Cd	107.9	
			Cd-Se(3)-Cd	90.1	
		Gap (eV)		1.79	1.87
$(CdSe)_{33}$	12 NH_3	Bond Length (Å)	Cd(4)-Se	2.668	
			Cd(3)-Se	2.629	
			Cd(3)-N	2.330	
(Figure 4c)		Angle (deg)	Se-Cd(4)-Se	109.3	
			Se-Cd(3)-Se	116.8	
			Cd-Se(4)-Cd	108.5	
			Cd-Se(3)-Cd	91.6	
		Gap (eV)		1.84	1.93
$(CdSe)_{33}$	21 NH_3	Bond Length (Å)	Cd(4)-Se	2.660	
			Cd(3)-Se	2.644	
			Cd(3)-N	2.339	
(Figure 4d)		Angle (deg)	Se-Cd(4)-Se	109.3	
			Se-Cd(3)-Se	116.1	
			Cd-Se(4)-Cd	108.6	
			Cd-Se(3)-Cd	92.7	
		Gap (eV)		2.07	2.10

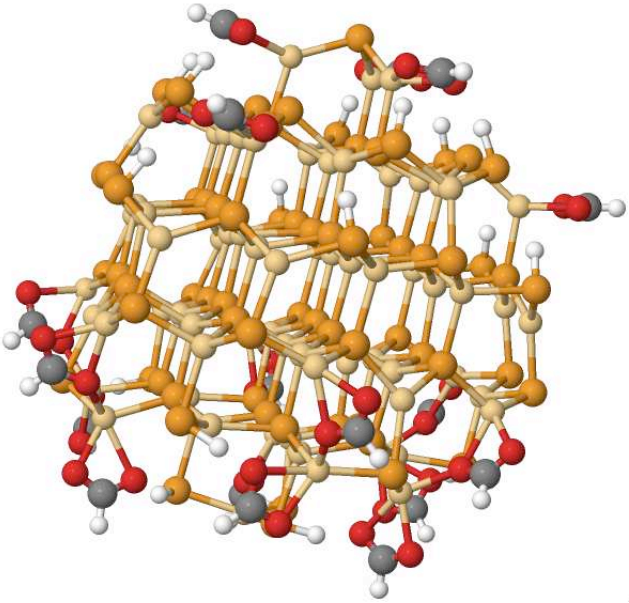

Figure 5: $(CdSe)_{66}$ cluster capped with 18 formate-hydrogen pairs.

group. The geometrical effect is related to the way of coordination, for which the two-coordinated Cd atom passes directly to a four-coordinated situation as in the case of the ideal wurtzite structure.

An important feature is highlighted in the case of the $(CdSe)_{33}$ capped both with the formate-hydrogen pair and with ammonia (Figure 3c); in this case the gap is the same as when only the formate-hydrogen pair is employed. This suggests that the HOMO and LUMO energies of the systems in which the two-coordinated Cd atoms are capped with the carboxylate-hydrogen pairs are influenced by the same amount due to the saturation of the three-coordinated Cd atoms, so that their energy difference remains constant. This does not mean that the higher and lower lying states are not influenced by that saturation.

In the cases in which only ammonia and methyl amine are used as capping agents, the geometry of the semiconductor part of the cluster resembles the bare cluster. In this case the HOMO-LUMO gap is only slightly larger than for the bare cluster ($\sim$0.15 eV). Only when all the surface cadmium atoms are capped with an ammonia (Figure 4d) the gap becomes wider by 0.4 eV compared to the bare cluster.

The bare $(CdSe)_{66}$ cluster is built up by placing the origin of the system on the midpoint of next nearest Cd and Se atoms along the *c* axes of the ideal wurtzite lattice (origin O3), resulting in a

diameter of $\sim$17 Å. Figure 5 shows the relaxed structure of the $(CdSe)_{66}$ capped cluster. From this ball and stick model it is possible to see that the inner part of the cluster has an atomic arrangement very close to the ideal wurtzite lattice structure. In this cluster some of the features of the wurtzite lattice are recognizable, such as the stacking of the hexagonal planes of the cations and anions and the characteristic tetrahedral coordination.

For this cluster the average angles for the four-coordinated cadmium and selenium atoms are 109.2° and 109.4° respectively, while the Cd-Se average bond length for the inner atoms is 2.641 Å. These results are close to those of the wurtzite CdSe bulk.

Comparing these results with those of the smaller clusters, it is possible to state that increasing the dimension, the structure of the inner part of the clusters becomes closer and closer to the ideal wurtzite structure. Nevertheless, even for the $(CdSe)_{66}$ cluster, the percentage of surface atoms is around 50%, so surface effects are still expected to strongly affect the overall cluster structure.

Binding Energies

In this section the interaction between the ligands and the CdSe cluster surface is analyzed, in terms of Binding Energies (BE) per ligand molecule. In this way it is possible to show that the ligands actually stabilize the cluster structure, providing a better saturation of the surface dangling bonds than the surface reconstruction alone.

The BE is given as the difference between the energy of the capped cluster and the sum of energies of the free (relaxed) ligands and the relaxed bare cluster, divided by the number of ligands.

This scheme is applicable to all clusters in which only one type of ligand is used as a capping agent.

Table 4 reports the BE for the ligands employed to cap the $(CdSe)_{33}$ cluster. The negative sign means that the interaction is a stabilizing contribution to the total energy of the system compared to the isolated bare cluster and ligands.

Comparing the clusters with the same number of ligands, ammonia generally displays a higher value of the BE. This is due to the fact that no bond breakings are involved in the interaction between

the ligands and the cluster surface. Note that increasing the number of ammonia from 9 to 21, results in a decrease of the average interaction energy as an effect of the congestion of the ligand molecules at the surface. These BE are consistent with previous calculations, at the LDA level, on the interaction between organic surfactant molecules and the surfaces of the CdSe semiconductor nanoparticles[21].

The exchange of formate with acetate and ammonia with methyl amine results in both cases in an increasing of the BE. It is likely due to the inductive effect of the methyl group that enhances the electron donor character of the ligand, so that it is more suitable to saturate the partial positive charge of the Cd surface atoms.

Calculated Photoabsorption Spectra

In this section the calculated TDDFT spectra are presented for some of the structures previously considered.

It is well known that usually the DFT ground state band gap of a solid structure is narrower than the experimental value. This problem is also evident in the calculated HOMO-LUMO gap of the CdSe clusters previously presented, for instance, in the case of the $(CdSe)_{33}$ cluster, that has an average diameter of 1.3 Å, the calculated GGA gap is $\sim$2.5 eV, whereas the experimental one is $\sim$3.0 eV.

Table 4: Average Binding Energy (BE) calculated for the $(CdSe)_{33}$ cluster. The numbers in parenthesis represent the number of ligands used as surfactant molecules for each $(CdSe)_{33}$ capped cluster.

Ligand	BE (kcal/mol)	
	LDA	GGA
Formate-Hydrogen pair (9)	-19.0	-10.1
Acetate-Hydrogen pair (9)	-25.0	-13.6
Ammonia (9)	-29.5	-18.8
Ammonia (12)	-25.9	-17.8
Ammonia (21)	-24.6	-16.5
Methyl Amine (9)	-30.6	-19.4

To deal with this problem, it is reasonable to assume that, for a given GGA potential, the electron self-interaction error is the same for the large model clusters and for the bulk system. Furthermore the goal of the calculations is not to predict the absolute energy scale of the spectrum, but rather to reproduce the spectrum on a relative energy scale, which can be corrected "a posteriori" by a constant energy shift. Therefore the band structure of the wurtzite bulk CdSe system has been calculated using the PW91 functional and the same basis sets for cadmium and selenium as employed for the cluster calculations: a calculated band gap of 1.31 eV was obtained, to be compared with the experimental value of 1.73 eV. So we assume that our scheme underestimates the band gap by 0.43 eV. Therefore all TDDFT transitions energies have been shifted upwards by 0.43 eV.

In Figure 7 the TDDFT spectra for the $(CdSe)_{33}$ clusters are reported. A common feature of these spectra is that they can be divided into two regions. In the first one, at relative low photon energies, the spectrum shape appears quite complicated with a structured series of peaks; in the second one, at higher photon energies, the absorption intensity seems to grow more or less monotonically.

It is important to notice that for all clusters the transitions in the low energy part of the calculated spectrum, when the photon energy is close to the HOMO-LUMO energy difference, are strongly dominated by a single occupied-virtual orbital excitation, which contributes up to the 98% of the overall transition. These transitions are therefore well described in the *independent particles approximation* (IPA) for which the transition is an excitation from a single occupied to a single virtual orbital.

Passing to the higher energy region this behavior becomes gradually less important, giving stronger mixing of configurations for each transition. Therefore the transitions become more and more congested as the photon energy increases. The progressive accumulation of transitions in the high energy region of the spectrum gives rise to a continuous growth of the absorption intensity.

This behavior can be interpreted with a solid state analogy. In the case of an insulator or semiconductor the exciton transitions are observed for photon energies slightly below the band gap of the system. These transitions are discrete, i.e. neat and well separated as in the case of the low

energy part of the cluster spectra (Figure 7). As soon as the photon energy becomes higher than the fundamental absorption edge, all the allowed band-to-band transitions between the valence and conduction bands take place, resulting in a strong increase in the absorption profile. This is also observed in the high energy region of the cluster spectra. However, we will focus on the lower energy region of the computed spectra, which may be associated with the exciton phenomena.

Since for the CdSe clusters, the first transitions of the spectra are properly described as single one-electron excited configurations, it is possible to characterize these excitations by looking at the occupied and virtual orbitals involved in the transitions (see also Table 5). For all clusters the occupied orbitals with energies close to the HOMO are linear combinations of surface selenium 4*p* orbitals, whereas the virtual orbitals in the vicinity of the LUMO are linear combinations of inner cadmium 5*s* orbitals (see also Figure 6).

The HOMO, HOMO-1 and HOMO-2 of the passivated $(CdSe)_{33}$ cluster are localized on the surface Se atoms, while the LUMO is essentially localized on Cd atoms of the inner part of the cluster. In all cases the orbitals do not contain appreciable contributions from the ligands. Such analysis in the case of the $(CdSe)_{33}$ cluster capped only with the formate-hydrogen pair, suggests that the exciton can be described as a charge transfer from surface selenium *p* states to inner cadmium *s* states.

A particular feature of the bare CdSe clusters electronic structure is that, usually, while the density of states near the HOMO is high, i.e. the HOMO, HOMO-1, HOMO-2, ... are close in energy with differences around $\sim$0.02 eV; the LUMO and LUMO+1 orbitals display an energy difference generally around 0.5 eV. This particular feature has been investigated by L. W. Wang and coworkers[32] using a pseudo potential approach. In their work it is shown that in the bulk CdSe, there is a density-of-states tail below the conduction-band minimum. In the quantum dot, this tail breaks into a few orbitals. For the smallest quantum dot, only one orbital is left in that energy region, resulting in a mid gap state, i.e. an isolated state between the top of the valence band and the bottom of the conduction band.

In the case of $(CdSe)_{33}$ also the spectrum of the cluster capped with the acetate-hydrogen pair

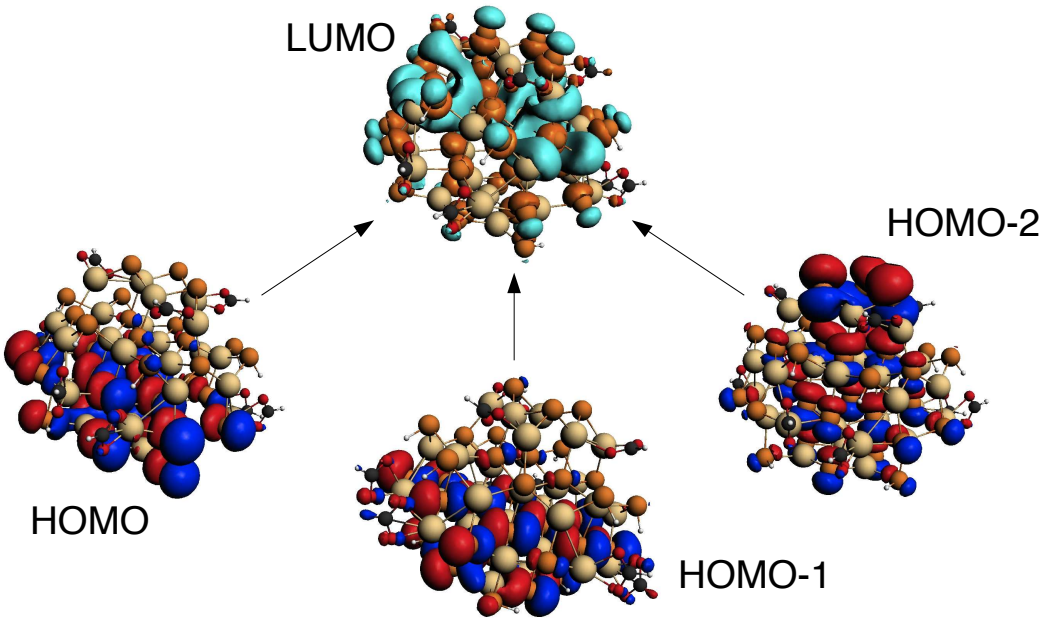

Figure 6: Orbitals mainly involved in the excitonic transition for the $(CdSe)_{33}$ cluster capped with only formate-hydrogen pair. The arrows symbolize the transition between the occupied to the virtual orbitals. Cd atoms light yellow, Se atoms bronze.

has been calculated (Figure 7c). No deviations are observed for the excitonic peak, while, at higher energy a broadening of the low intensity resonances is observed.

Figure 7 e-h show the TDDFT spectra of the $(CdSe)_{33}$ clusters capped only with ammonia or methyl amine: the obtained shapes are very different from those found in clusters protected by the carboxylate-hydrogen pairs.

The main difference in the absorption spectrum between $(CdSe)_{33}$ cluster capped with donor ligands and with the carboxylate-hydrogen pairs, is that, in the second case the absorption profile starts around an energy of 3.0 eV, $\sim$0.5 eV higher than in the first case. This is probably due to the stronger bonding of the carboxylate-hydrogen pairs with the surface atoms.

This higher efficiency in saturating the dangling bonds of the formate and acetate groups can be related to electronic and geometric effects. The electronic effect regards the negative charge of the oxygen in the carboxylic group, that can stabilize better than the amino group, the partially positive unsaturated cadmium atoms. The geometrical effect is related to the coordination, i.e. the two-coordinated Cd surface atom needs only one molecule to create a four-coordinated situation as

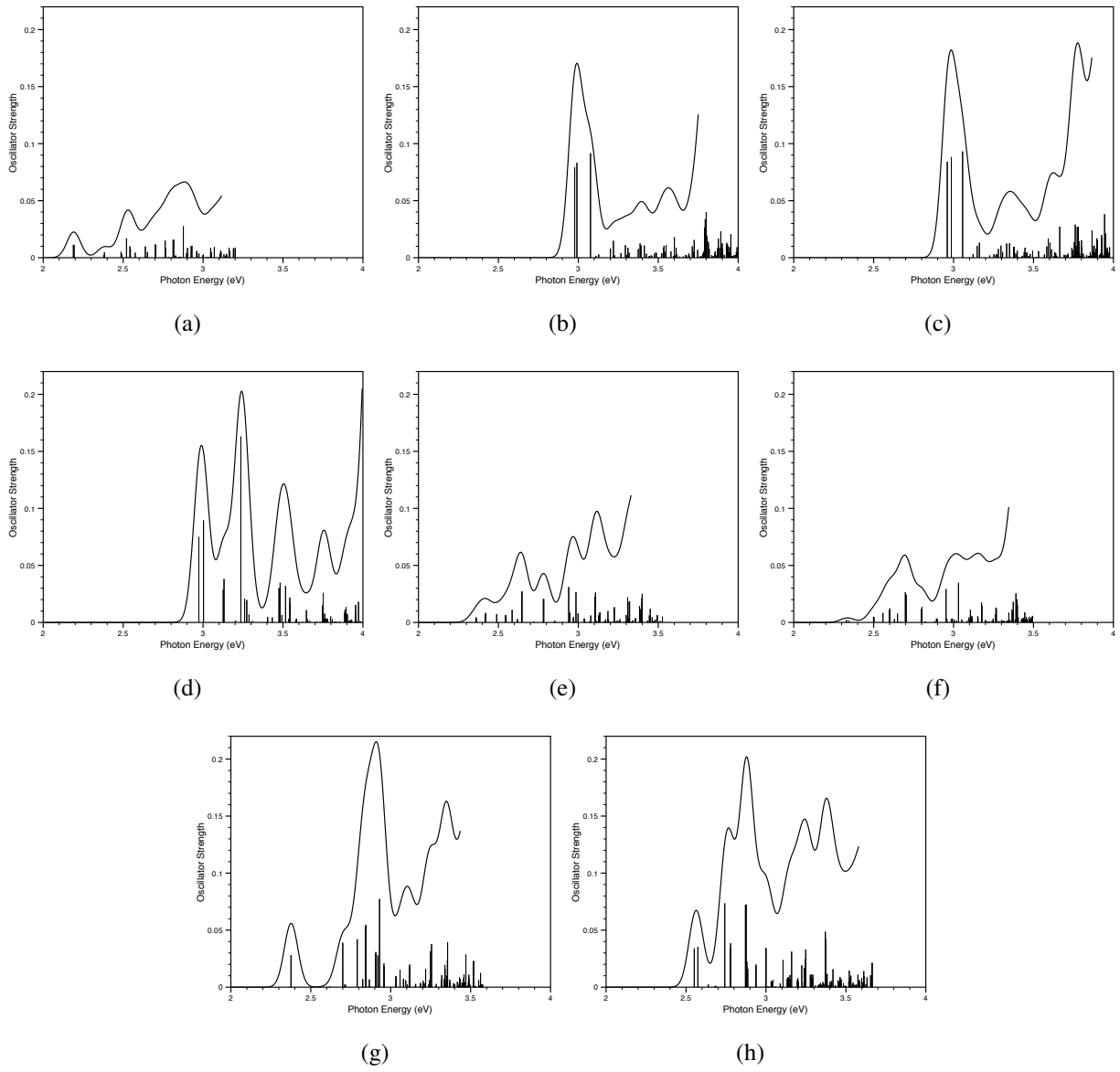

Figure 7: TDDFT spectra for the $(CdSe)_{33}$ model clusters. a) Bare $(CdSe)_{33}$ (Figure 1). b) $(CdSe)_{33}$ with 9 formate-hydrogen pairs (Figure 3a). c) $(CdSe)_{33}$ with 9 acetate-hydrogen pairs (Figure 3b). d) $(CdSe)_{33}$ with 9 formate-hydrogen pairs and 12 NH_3 (Figure 3c). e) $(CdSe)_{33}$ with 9 NH_3 (Figure 4a). f) $(CdSe)_{33}$ with 9 methyl-amines (Figure 4b). g) $(CdSe)_{33}$ with 12 NH_3 (Figure 4c). h) $(CdSe)_{33}$ with 21 NH_3 (Figure 4d). All spectra have been shifted by +0.43 eV.

in the case of the ideal wurtzite structure.

Substitution of ammonia by methyl amine results in a reduction of the oscillator strengths of the transitions in a non homogeneous way. Consequently, a different spectrum profile is obtained for the two cases, even though the excitation energies are hardly influenced by this substitution.

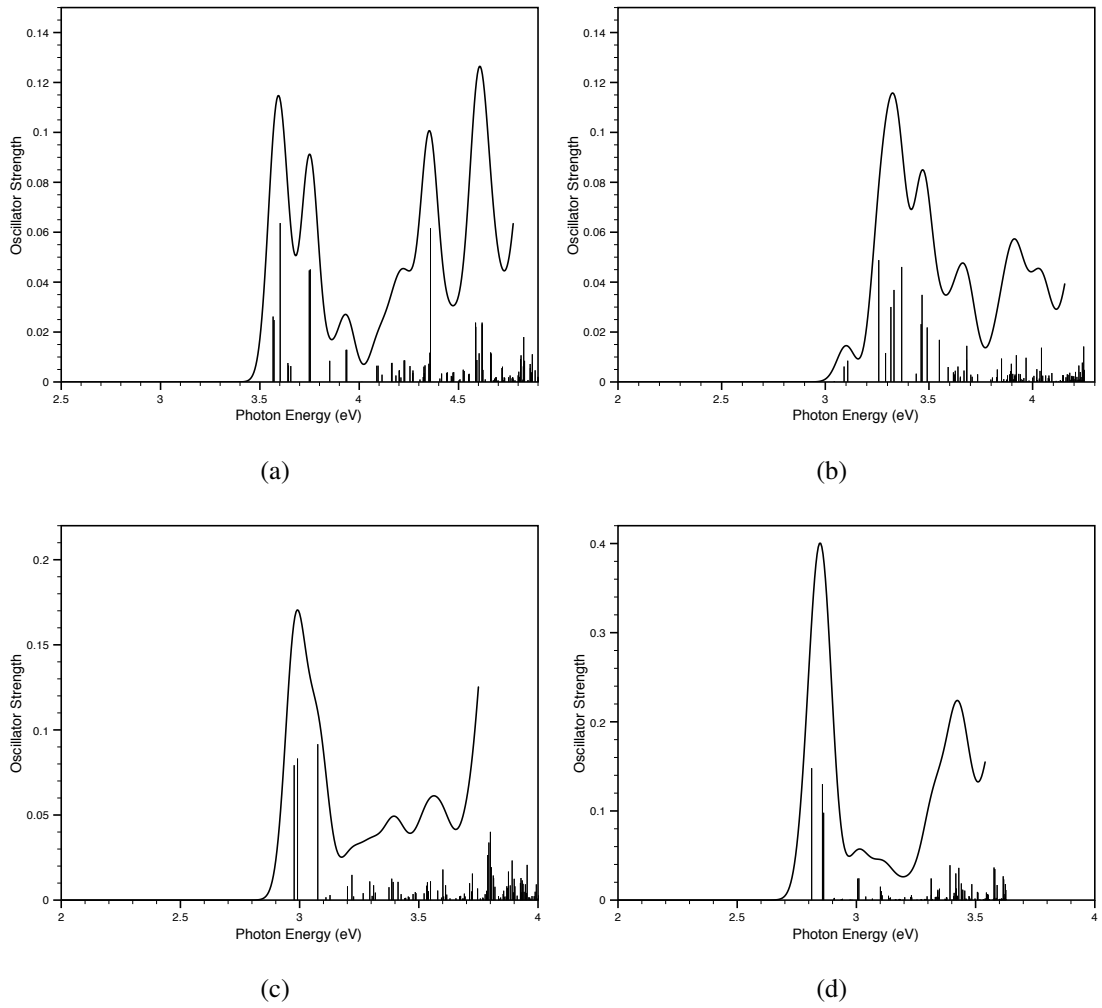

Figure 8: TDDFT spectra for the $(CdSe)_n$ model clusters capped by the formate-hydrogen pairs. a) $(CdSe)_{13}$ with 6 formate-hydrogen pairs (2a). b) $(CdSe)_{19}$ with 6 formate-hydrogen pairs (2b). c) $(CdSe)_{33}$ with 9 formate-hydrogen pairs (Figure 3a). d) $(CdSe)_{66}$ with 18 formate-hydrogen pairs (Figure 5). All spectra have been shifted by +0.43 eV.

Focusing on the clusters capped only with the formate-hydrogen pair Figure 8, it is possible to notice that the enlargement of the cluster results in a red-shift of the spectra, and an increase in the oscillator strength. While for the small $(CdSe)_{13}$ and $(CdSe)_{19}$ clusters (Figures 8a and 8b), the spectra have a rather complicated shape, in the case of $(CdSe)_{33}$ and $(CdSe)_{66}$ (Figures 8c and 8d), the spectrum shows one clear peak just at the beginning, without any other pronounced resonances at higher energy. The two spectra are very similar in shape, and in this case, the bathochromic and hyperchromic effects passing from $(CdSe)_{33}$ to $(CdSe)_{66}$ are very evident. A common feature of the

two cluster spectra is that the first peak (the excitonic peak), consists of only three strong transitions that originate respectively from the HOMO, HOMO-1 and HOMO-2, to the LUMO.

The inner semiconductor parts of both $(CdSe)_{33}$ and $(CdSe)_{66}$ have an atomic arrangement very close to the wurtzite ideal structure (see Figures 3a and Figure 5). For the smaller $(CdSe)_{13}$ and $(CdSe)_{19}$ clusters this is not true, due to the higher number of surface atoms that strongly affect the inner part of the cluster. Probably for this reason the spectrum profile for these structures does not match with the shape obtained for the larger clusters, even though, in both cases, an intense peak is still appreciable at the lower end of the spectrum.

Since $(CdSe)_{33}$ capped with formate-hydrogen pairs will be employed as a reference for comparison with experimental data in the next section, we have analyzed the most intense transitions in Table 5, where the excitation energy, the oscillator strength and the excited state composition have been reported. It is worth noting that all the excitations correspond to transitions from Se 4*p* to Cd 4*s*. Moreover, while the excitons at 2.98 -3.08 eV are all well described as single monoexcited configurations (>98%), higher lying excitations consist in general of various configurations.

Table 5: Valence Excitation Spectrum of $(CdSe)_{33}$ cluster capped with formic acid (Figure 7b and 8c). In the Table, shifted excitation energy (E_{exc}), oscillator strength (f), and excited-state composition in terms of mono-excited configurations are reported. Only the transitions with $f > 0.02$ are shown. The main contributions to the initial and final orbitals are reported in parenthesis. Only the mono-excited configurations that contribute more than 10% are reported.

excitation	E_{exc}(eV)	f	excited state composition		
1	2.98	0.0792	98% HOMO (Se 4p 100%)	→	LUMO (Cd 5s 95%, Se 4p 5%)
2	2.99	0.0832	99% HOMO-1 (Se 4p 100%)	→	LUMO
3	3.08	0.0916	99% HOMO-2 (Se 4p 100%)	→	LUMO
59	3.80	0.0401	34% HOMO-1	→	LUMO+3 (Cd 5s 94%, Se 4p 6%)
			18% HOMO-12 (Cd 5p 3%, Se 4p 97%)	→	LUMO+1 (Cd 5s 90%, Se 4p 10%)
			14% HOMO-10 (Cd 5p 2%, Se 4p 98%)	→	LUMO+2 (Cd 5s 87%, Se 4p 13%)
			10% HOMO-12	→	LUMO+2

Comparison with Experiment

Since the diameters of the clusters are below 2 nm, these nanocrystals are in the magic size region: two of the most important works for the CdSe nanoparticles in this size regime are those reported by Kudera et al.[33] and Kasuya et al.[16].

Kudera deals with the sequential synthesis in solution of a series of magic size clusters. The actual capping of the clusters is not known, but the presence of nonanoic acid during the synthesis and the good agreement between the experimental and calculated spectra for the formate-hydrogen pair endcapped clusters suggest that these clusters are present. Therefore, in this section, only the results related to that kind of capped clusters are discussed.

Figure 9 shows the evolution of the UV-Vis absorption spectra in time. The position of the individual exciton peaks remain almost constant over time and only vary amplitude. Kudera et al. associate these results with the sequential appearance of different sizes. Figure 9a shows clearly the persistence over time of the peaks at 350-360 nm, 384 nm, 406 nm, and 431 nm, that are highlighted in the spectrum by vertical dashed lines. According to Kudera et al.[33], each line corresponds to a different family of magic size clusters.

Figure 9b shows the calculated exciton peaks for the $(CdSe)_n$, n=13, 19, 33 and 66 clusters. As it has been noticed in the previous section, increasing the size of the clusters results in a red-shift, as well as, an enhancement in the absorption intensity of the exciton peak.

Comparing the experimental and the calculated spectra in Figure 9, a good agreement is found. The position of the peak for each cluster is close to one of the vertical dashed lines. From these results it is reasonable to assume that the four families experimentally observed, would be related to the four clusters modelled in this work. In particular the following assignments can be done: (peaks at 350-360 nm) $\rightarrow$ $(CdSe)_{13}$; (peak at 384 nm) $\rightarrow$ $(CdSe)_{19}$; (peak 406 nm) $\rightarrow$ $(CdSe)_{33}$ and (peak 431 nm) $\rightarrow$ $(CdSe)_{66}$.

It is important to notice that the spectra collected during the synthesis, are the results of an overlap of the absorption profile of the families of cluster present at a certain time. This overlap would slightly change the positions of the peaks: the peak around 350 nm, at the early stages of the

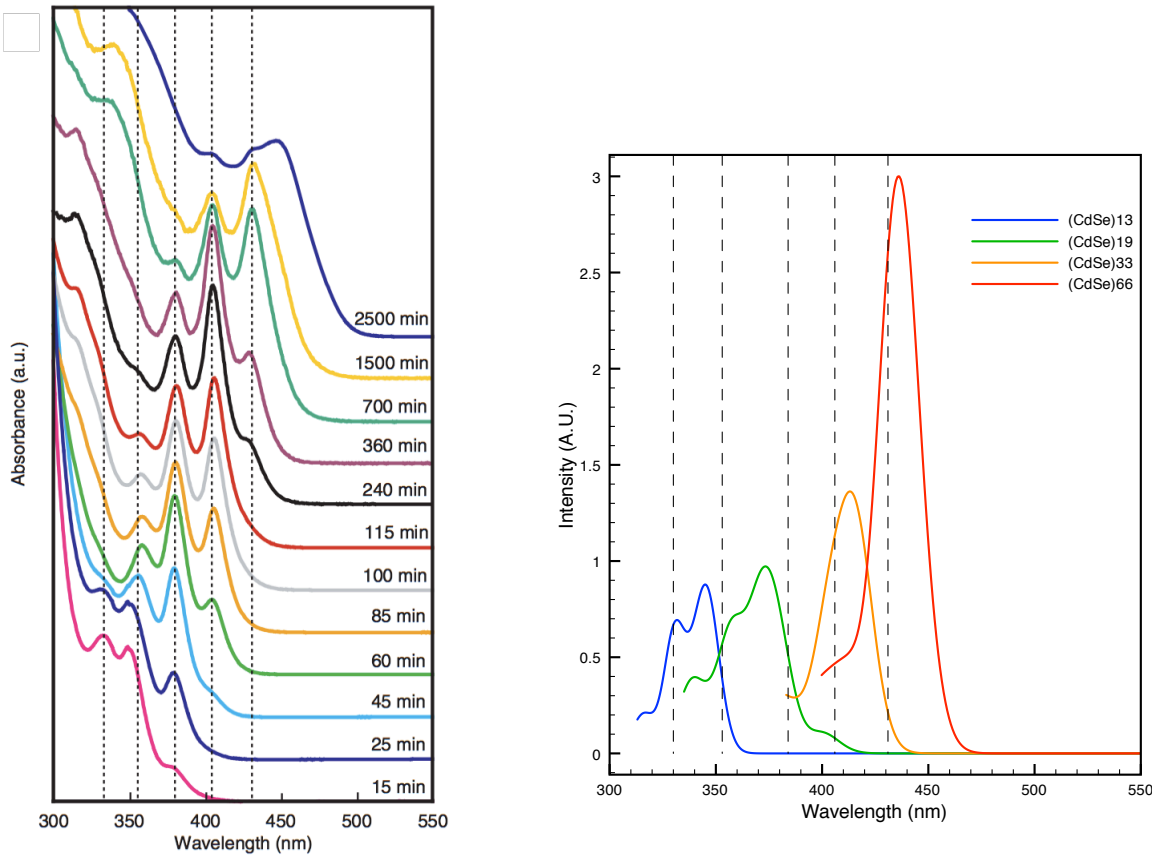

(a) (b)

Figure 9: Size evolution of CdSe nanocrystals. a) Absorption spectra of aliquots taken at different time during the synthesis of magic size clusters of CdSe (reproduced with permission, taken from[33]). b) Calculated TDDFT spectra of the $(CdSe)_n$ series. Only the exciton peak is shown. The vertical dashed lines are in the same position for both spectra. Calculated spectra have been shifted by +0.43 eV.

synthesis, is slightly below the vertical dashed line and then red-shifts to its final position (Figure 9a). This behavior is consistent with the overlap of the $(CdSe)_{13}$ and $(CdSe)_{19}$ calculated spectra. In fact the first peak in the $(CdSe)_{13}$ cluster spectra is slightly below the dashed line, while the first peak, in the case of $(CdSe)_{19}$, shows a shoulder close to the same line. If the overlap of these spectra is taken into account and considering the change in the relative intensity during the nanocrystals growth, the shift of the peak around 350 nm can be rationalized.

Kasuya[16] reported on the synthesis and identification of mass-selected $(CdSe)_{33}$ and $(CdSe)_{34}$ nanoparticles in solution. Curve 1 in Figure 10a shows the experimental spectrum of a solution

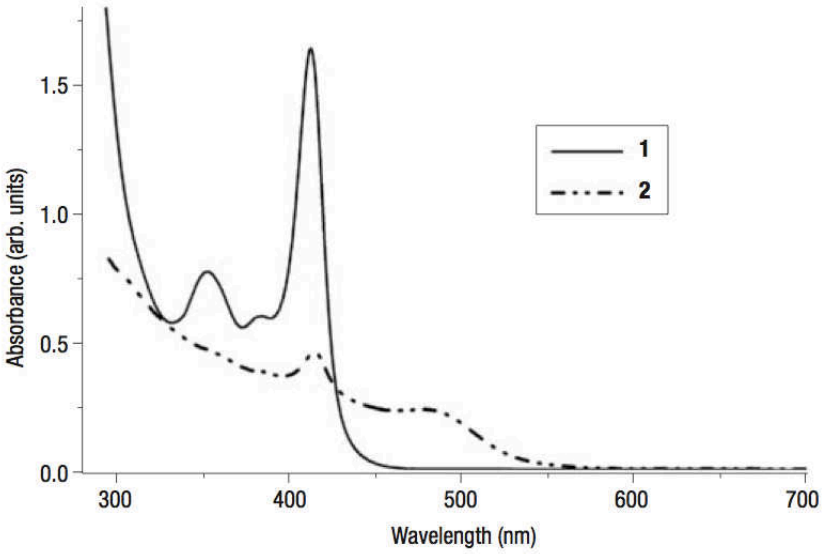

(a)

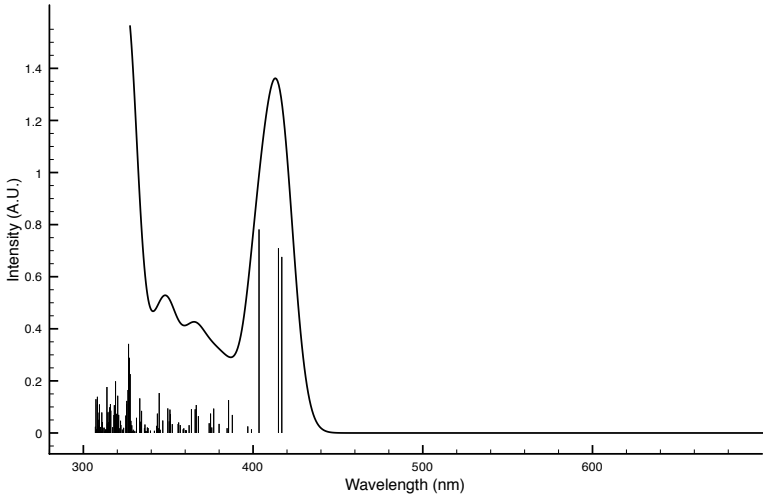

(b)

Figure 10: a) Optical absorption spectra of a solution containing $(CdSe)_{33}$ and $(CdSe)_{34}$ nanoparticles (Curve 1) (reprinted by permission from Macmillan Publishers Ltd: *Nature Materials*[16], copyright 2004). b) Calculated TDDFT spectrum of $(CdSe)_{33}$ cluster capped by formic acid (figure 3a). Calculated spectra have been shifted by +0.43 eV.

containing mainly $(CdSe)_{33}$ nanocrystals, identified by mass spectroscopy[16]. The calculated spectrum shows a good agreement for the excitonic peak and for the shape of the spectrum (Figure 10b). Moreover the TDDFT spectra display very similar features to that obtained experimentally for magic size cysteine-capped CdSe nanoparticles synthesized in aqueous solution[19,20].

The calculated TDDFT spectra are in line with those obtained experimentally for clusters with the same size. This suggests that the proposed structures are realistic models of the actual quantum dots.

Conclusion

In this work, the bare nanoparticles are built up considering only stoichiometric CdSe clusters obtained cutting an almost spherical portion of the ideal wurtzite lattice with experimental bulk Cd-Se bond lengths, according to the magic-size series reported by Kasuya et al.[16], that is $(CdSe)_n$, n=13, 19, 33 and 66.

To simulate the interaction between the bare clusters and the surfactants molecules, various model types of ligands are introduced. Therefore, for a proper design of the model clusters, it has proven necessary to allow structural relaxation and to employ carboxylate ligands.

Focusing on the TDDFT spectra calculated for the clusters capped only with the formate-hydrogen pair, it is possible to notice that increasing the dimension of the cluster results in a red-shift of the spectra, and an increase in the absorption intensity. In particular in the case of the $(CdSe)_{33}$ and $(CdSe)_{66}$, each spectrum shows a clear peak in the low energy region, without other pronounced features at higher energy.

These two spectra are very similar in shape, and in this case, it is evident the bathochromic and iperchromic effect that is observed passing from the $(CdSe)_{33}$ to the $(CdSe)_{66}$ cluster.

The best match between the calculated and experimental spectra has been achieved for the clusters capped only with the formate-hydrogen pair. For these spectra the comparison with the experiment has shown a good agreement for nanocrystals with the same dimension and capped with the same type of ligands, this suggests that the proposed structures are realistic models of the actual quantum dots.

In the case of the $(CdSe)_{33}$ cluster capped only with the formate-hydrogen pair, the excitonic peak is made up of only three strong transitions which start respectively from the HOMO, HOMO-1 and HOMO-2 orbitals and go to the LUMO orbital. All these three transitions can be described as charge transfers from surface selenium *p* states to inner cadmium *s* states.

Since this approach has given good results for the CdSe nanoparticles, it will be possible to extend the present computational protocol to other semiconductor nanocrystals. This will furnish a more complete description of the exciton nature that would come out from the comparison among

different systems.

In conclusion, this work has shown that current implementation of DFT and TDDFT methods are suitable to study optical properties of CdSe nanoclusters. The model cluster design (ligands nature and structural relaxation) is a very important and delicate choice, while the availability of large super computer facilities exploited by parallel computer codes allows to take into account large systems with a realistic size.

Acknowledgements

This work has been supported by MIUR (Programmi di Ricerca di Interesse Nazionale PRIN 2006 and 2008) of Italy, by INSTM (Progetto PRISMA 2004) and by DEMOCRITOS CNR-IOM National Simulation Center, Trieste, Italy. The work has been performed under the HPC-EUROPA2 project (project number: 228398) with the support of the European Commission - Capacities Area - Research Infrastructures and NCF. Remco W. A. Havenith acknowledges the Netherlands Organisation for Scientific Research (NWO/ECHO), grant 700.57.027 for financial support.

References

(1) Parak, W. J.; Gerion, D.; Pellegrino, T.; Zanchet, D.; Micheel, C.; Williams, S. C.; Boudreau, R.; Le Gros, M. A.; Larabell, C. A.; Alivsatos, A. P. Biological applications of colloidal nanocrystals. *Nanotechnology* **2003**, *14*, R15.

(2) Murray, C. B.; Noms, D. J.; Bawendi, M. G. Synthesis and Characterization of Nearly Monodisperse CdE (E = S, Se, Te) Semiconductor Nanocrystallites. *J. Am. Chem. Soc.* **1993**, *115*, 8706–8715.

(3) Brus, L. E. Electron-electron and electron-hole interactions in small semiconductor crystallites: The size dependence of the lowest excited electronic state. *J. Chem. Phys.* **1984**, *80*, 4403.

(4) Kilina, S.; Ivanov, S.; Tretiak, S. Effect of Surface Ligands on Optical and Electronic Spectra of Semiconductor Nanoclusters. *J. Am. Chem. Soc.* **2009**, *131*, 7717–7726.

(5) Puzder, A.; Williamson, A. J.; Gygi, F.; Galli, G. Self-Healing of CdSe Nanocrystals: First-Principles Calculations. *Phys. Rev. Lett.* **2004**, *92*, 217401.

(6) del Puerto, M. L.; Tiago, M. L.; Chelikowsky, J. R. Excitonic Effects and Optical Properties of Passivated CdSe Clusters. *Phys. Rev. Lett.* **2006**, *97*, 096401.

(7) Inerbaev, T. M.; Masunov, A. E.; Khondaker, S. I.; Dobrinescu, A.; Plamadă, A.-V.; Kawazoe, Y. Quantum chemistry of quantum dots: Effects of ligands and oxidation. *J. Chem. Phys.* **2009**, *131*, 044106.

(8) Shiang, J. J.; Kadavanich, A. V.; Grubbs, R. K.; Alivisatos, A. P. Symmetry of Annealed Wurtzite CdSe Nanocrystals: Assignment to the C_{3v} Point Group. *J. Phys. Chem.* **1995**, *99*, 17417–17422.

(9) Rosenthal, S. J.; McBride, J.; Pennycook, S. J.; Feldman, L. C. Synthesis, surface studies, composition and structural characterization of CdSe, core/shell and biologically active nanocrystals. *Surface Science Reports* **2007**, *62*, 111–157.

(10) Liu, H.; Owen, J. S.; Alivisatos, A. P. Mechanistic Study of Precursor Evolution in Colloidal Group II-VI Semiconductor Nanocrystal Synthesis. *J. Am. Chem. Soc.* **2007**, *129*, 305–312.

(11) Deng, Z.; Li Cao,; Tang, F.; Zou, B. A New Route to Zinc-Blende CdSe Nanocrystals: Mechanism and Synthesis. *J. Phys. Chem. B* **2005**, *109*, 16671–16675.

(12) von Holt, B.; Kudera, S.; Weiss, A.; Schrader, T. E.; Manna, L.; Parak, W. J.; Braun, M. Ligand exchange of CdSe nanocrystals probed by optical spectroscopy in the visible and mid-IR. *J. Mater. Chem.* **2008**, *18*, 2728–2732.

(13) Bowen Katari, J. E.; Colvin, L. V.; Alivisatos, A. P. X-ray Phothoelectron Spectroscopy of CdSe Nanocrystals with Applications to Studies of the Nanocrystal Surface. *J. Phys. Chem.* **1994**, *98*, 4109–4117.

(14) Winkler, U.; Eich, D.; Chen, Z. H.; Fink, R.; Kulkarni, S. H.; Umbach, E. Detailed investigation of CdS nanoparticle surfaces by high-resolution photoelectron spectroscopy. *Chem. Phys. Lett.* **1999**, *306*, 95–102.

(15) Bouldin, C. E.; Bell, M. I.; Kemner, K. M.; Woicik, J. C.; Majetich, S. A.; Carter, A. C. Surface structure of cadmium selenide nanocrystallites. *Phys. Rev. B* **1997**, *55*, 13822.

(16) Kasuya, A. et al. Ultra-stable nanoparticles of CdSe revealed from mass spectroscopy. *Nature Materials* **2004**, *3*, 99.

(17) Kuçur, E.; Ziegler, J.; Nann, T. Synthesis and Spectroscopic Characterization of Fluorescent Blue-Emitting Ultrastable CdSe Clusters. *Small* **2008**, *4*, 883–887.

(18) Ptatschek, V. et al.Ptatschek, V. and others Quantized aggregation phenomena in II-VI semiconductor colloids. *Ber. Bunsenges. Phys. Chem.* **1998**, *102*, 85–95.

(19) Yeon-Su, P.; Dmytruk, A.; Dmitruk, I.; Kasuya, A.; Okamoto, Y.; Kaji, N.; Tokeshi, M.; Baba, Y. Aqueous Phase Synthesized CdSe Nanoparticles with Well-Defined Numbers of Constituent Atoms. *J. Phys. Chem. C* **2010**, *114*, 18834.

(20) Yeon-Su, P.; Dmytruk, A.; Dmitruk, I.; Kasuya, A.; Takeda, M.; Ohuchi, N.; Okamoto, Y.; Kaji, N.; Tokeshi, M.; Baba, Y. Size-Selective Growth and Stabilization of Small CdSe Nanoparticles in Aqueous Solution. *ACS Nano* **2010**, *4*, 121.

(21) Puzder, A.; Williamson, A. J.; Zaitseva, N.; Galli, G. The Effect of Organic Ligand Binding on the Growth of CdSe Nanoparticles Probed by Ab Initio Calculations. *Nano Lett.* **2004**, *4*, 2361–2365.

(22) Kim, H.-S.; Jang, S.-W.; Chung, S.-Y.; Lee, S. Effects of Bioconjugation on the Structures and Electronic Spectra of CdSe: Density Functional Theory Study of CdSe-Adenine Complexes. *J. Phys. Chem. B* **2010**, *114*, 471.

(23) Nguyen, K. A.; Day, P. N.; Pachter, R. Understanding Structural and Optical Properties of Nanoscale CdSe Magic-Size Quantum Dots: Insight from Computational Prediction. *J. Phys. Chem. C* **2010**, *114*, 16197–16209.

(24) Yu, M.; Fernando, G. W.; Li, R.; Papadimitrakopoulos, F.; Shi, N.; Ramprasad, R. First principles study of CdSe quantum dots: Stability, surface unsaturations, and experimental validation. *App. Phys. Lett.* **2006**, *88*, 231910.

(25) Deglmann, P.; Ahlrichs, R.; Tsereteli, K. Theoretical studies of ligand-free cadmium selenide and related semiconductor clusters. *J. Chem. Phys.* **2002**, *116*, 1585.

(26) Fonseca Guerra, C.; Snijders, J. G.; te Velde, G.; Baerends, E. J. Towards an order-N DFT method. *Theoretical Chemistry Accounts* **1998**, *99*, 391.

(27) Vosko, S. H.; Wilk, L.; Nusair, M. Accurate spin-dependent electron liquid correlation energies for local spin density calculations: a critical analysis. *Canadian Journal of Physics* **1980**, *58*, 1200.

(28) Perdew, J.; Chevary, J.; Vosko, S.; Jackson, K.; Pederson, M.; Sing, D.; Fiolhais, C. Atoms,

molecules, solids, and surfaces: Applications of the generalized gradient approximation for exchange and correlation. *Phys. Rev. B* **1992**, *46*, 6671.

(29) van Leeuwen, R.; Baerends, E. J. Exchange-correlation potential with correct asymptotic behavior. *Phys. Rev. A* **1994**, *49*, 2421–2431.

(30) te Velde, G.; Baerends, E. J. Precise density-functional method for periodic structures. *Phys. Rev. B* **1991**, *44*, 6721.

(31) Rempel, J. Y.; Trout, B. L.; Bawendi, M. G.; Jensen, K. F. Properties of the CdSe(0001), (000$\bar{1}$), and (11$\bar{2}$0) Single Crystal Surfaces: Relaxation, Reconstruction, and Adatom and Admolecule Adsorption. *J. Phys. Chem. B* **2005**, *109*, 19320–19328.

(32) Wang, L. W.; Zunger, A. Pseudopotential calculations of nanoscale CdSe quantum dots. *Phys. Rev. B* **1996**, *53*, 9579.

(33) Kudera, S.; Zanella, M.; Giannini, C.; Rizzo, A.; Li, Y.; Gigli, G.; Cingolani, R.; Ciccarella, G.; Spahl, W.; Parak, W. J.; Manna, L. Sequential Growth of Magic-Size CdSe Nanocrystals. *Adv. Mater.* **2007**, *19*, 548–552.